Preprint Title	Study of tribenzo[b,d,f]azepine as donor in D-A photocatalysts.
Authors	Katy Medrano-Uribe, Jorge Humbrías-Martín and Luca Dell'Amico
Publication Date	19 Feb. 2025
Article Type	Full Research Paper
Supporting Information File 1	Tribenzoazepine as donor in organic photocatalysts with D-A structure (Supporting information).pdf; 3.9 MB
ORCID® iDs	Katy Medrano-Uribe - https://orcid.org/0000-0001-9801-9524; Jorge Humbrías-Martín - https://orcid.org/0000-0002-0245-727X; Luca Dell'Amico - https://orcid.org/0000-0003-0423-9628

Study of tribenzo[b,d,f]azepine as donor in D-A photocatalysts.

Katy Medrano-Uribe*[1], Jorge Humbrías-Martín[1], and Luca Dell'Amico*[1]

Address:[1]Department of Chemical Sciences, University of Padova, Via Francesco Marzolo 1, 35131, Padova (Italy).

Email: Luca Dell'Amico – luca.dellamico@unipd.it

   Katy Medrano-Uribe – katyelizabeth.medranouribe@unipd.it

* Corresponding author

Abstract

Since the discovery of donor-acceptor (D-A) type molecules in the field of material science, they have found great applicability in the field of photocatalysis. Most of these compounds are based on complex D-A-D structures or multi-D-A systems, such as the 4CzIPN. Whereas these systems have been widely studied and applied as photocatalysts, simpler D-A structures remain less explored. Nevertheless, the simplicity of D-A structures makes them the ideal structures to further understand the structure-property relationship of donor-acceptor (D-A) molecules for optimizing their photocatalytic performance by simpler modification of the different D-A subunits. In particular, D-A structures featuring sulfur-based acceptors and nitrogen donors have gained increasing attention for their use as photoredox catalysts. This study introduces a new family of D-A molecules by exploring various sulfur-based acceptors and nitrogen donors, including a novel tribenzo[b,d,f]azepine (TBA) unit and 5H-dibenz[b,f]azepine (IMD). Our findings demonstrate that these simple D-A structures exhibit promising photocatalytic properties, comparable to those of more complex D-A-D systems.
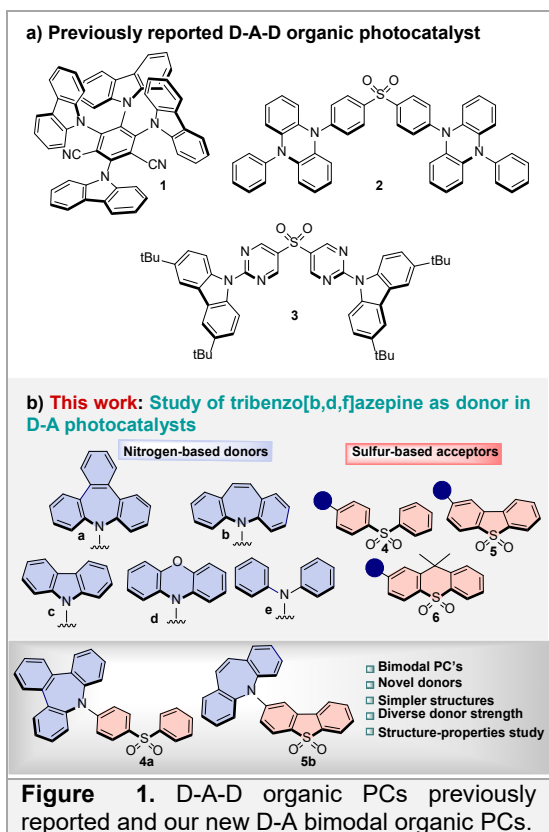
Keywords

donor-acceptor system; photoredox catalysis; organic photocatalyst; photocatalyst design

Introduction

In recent years, photocatalysis has emerged as a powerful tool for the construction and functionalization of organic molecules and materials. Thus, the scientific community has focused on the design and study of new organic molecules that can be used as photocatalysts, replacing generally more expensive metal-based complexes.[1a-c] Furthermore, there is a particular interest in the obtention of organic molecules with well-balanced redox potentials in the excited state that can be act as bimodal photocatalyst, facilitating their use in oxidative and reductive quenching cycles. In this sense, it is crucial to understand the molecule's structure-properties dependence to modulate its optical and photoredox properties.[2] For instance, molecules with donor-acceptor (D-A) structures, classically used as OLED emitters, have gained relevance by finding alternative applications in the field of photocatalysis.[3] In this type of structure, the electron density distribution in the charge transfer (CT) excited state is facilitated for the presence of an electron-rich moiety and an electron-poor part in the same molecule, increasing the lifetime in the excited state. One of the representative class of molecules demonstrating a dual use in material chemistry and photocatalysis is the carbazolyl dicyanobenzene (CDCB) family. Since the initial report on the synthesis and photoluminescence study of 4CzIPN (**1,** Figure 1a),[4] the scientific community has recognized its potential under photocatalytic manifolds. This interest is attributed to: i) its absorption profile in the visible region, ii) a long lifetime of the excited states, and iii) balanced redox potentials in both the ground and excited states.[5] In 2018, Zeitler and her collaborators conducted an innovative and in-depth study on modulating the photochemical properties of a family of donor-acceptor cyanoarenes.[6] They employed various nitrogen donor molecules attached to diversely substituted acceptor cores. This systematic approach allowed the authors to develop new organic photocatalysts (PCs) with strong reductive or oxidative properties based on the different redox potentials.

Although diverse scaffolds have been reported in the literature, the identification and use of novel PCs with tunable and diverse optical and redox properties can pave the way to uncharted reactivity. In this context, sulfur-based cores, widely used as acceptors in photoelectric materials,[7a-f] and dyes[8a,b] serve as promising structures for constructing and designing novel PCs. These structures show a high electron affinity, stability, and the possibility of tuning their physicochemical properties by substituting the two aromatic rings. In 2018, Sang Kwon and co-workers reported a computational study to design new PCs to be employed in atom transfer radical polymerization (O-ATRP).[9] Notably, the sulfur-based structure **2** showed excellent performances for this transformation. One year later, the same research group reported its use in a reversible addition-fragmentation chain-transfer (RAFT) polymerization.[10] Moreover, in 2022, Zysman and collaborators showed that molecule **3**, initially synthesized as TADF (thermally activated delayed fluorescence) emitter,[7f] can be used as a PC under electron-transfer (ET) and energy-transfer (EnT) processes (Figure 1a) .[11] All the main reports in the field focused on D-A-D (donor-acceptor-donor) structures. Quite surprisingly, the potential use as PCs of structurally simpler D-A molecules have been largely overlooked.

a) Previously reported D-A-D organic photocatalyst

b) **This work**: Study of tribenzo[b,d,f]azepine as donor in D-A photocatalysts

Nitrogen-based donors

Sulfur-based acceptors

- Bimodal PC's
- Novel donors
- Simpler structures
- Diverse donor strength
- Structure-properties study

**Figure 1.** D-A-D organic PCs previously reported and our new D-A bimodal organic PCs.

Aliphatic and aromatic nitrogen donors are widely used in synthesizing fluorescent emitters due to their electron-donating strength. The development of stronger donors to enhance luminescence remains a key area of research.[12] Recently, azepine-based analogs, such as tribenzo[b,d,f]azepine (TBA, **a**), have been explored due to their photoluminescence properties.[13a-e] This antiaromatic core offers unique features, including twisted structures, reduced π-π stacking, and enhanced reverse intersystem crossing rates. Similarly, 5H-Dibenz[b,f]azepine (IMD, **b**) has been incorporated into D-A-D structures, showing interesting photophysical properties compared to common substrates like carbazole (**c**), diphenylamine (**d**), and phenoxazine (**e**).[14a-c] However, their potential as D-unit in organic PCs remains unexplored. For this reason, studying this avenue could unlock new opportunities for the synthesis and design of more powerful, efficient and versatile organic photocatalysts.

We herein present the design, synthesis and study of a new sulfur-based D-A family using diverse nitrogen donors (Figure 1b). We performed complete photophysical characterization of the diverse D-A molecules to analyze the structure-properties relationships. We furher studied their photocatalytic potential as bimodal PCs and demonstrated their potential use in different reductive and oxidative quenching processes.

Results and Discussion

Photophysical properties analysis.

We started our study with three different sulfur-based acceptors, namely: diphenyl sulfone (**4**), dibenzo[*b,d*]thiophene 5,5-dioxide (**5**), and 9,9-dimethyl-9*H*-thioxanthene 10,10-dioxide (**6**). The selection of these scaffolds was aimed at investigating the effect of conjugation and rigidity/flexibility on the presence of the same donor (TBA, **a**). In the case of the D-A compounds **4a** and **6a**, we observed a blue-shifted absorption profile due to the break of the conjugation in sulfur-based acceptors. Compounds **4a** and **6a** presented a similar absorption profile, while molecule **5a** showed a red-shifted spectrum tailing up to the visible region (Figure 2a).
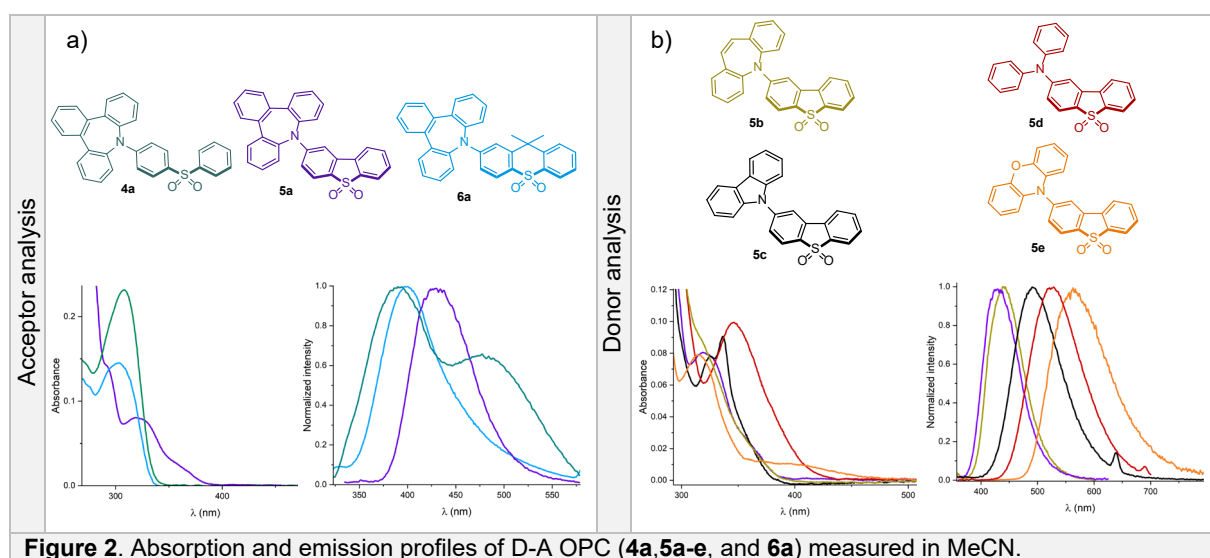
Figure 2. Absorption and emission profiles of D-A OPC (**4a**,**5a-e**, and **6a**) measured in MeCN.
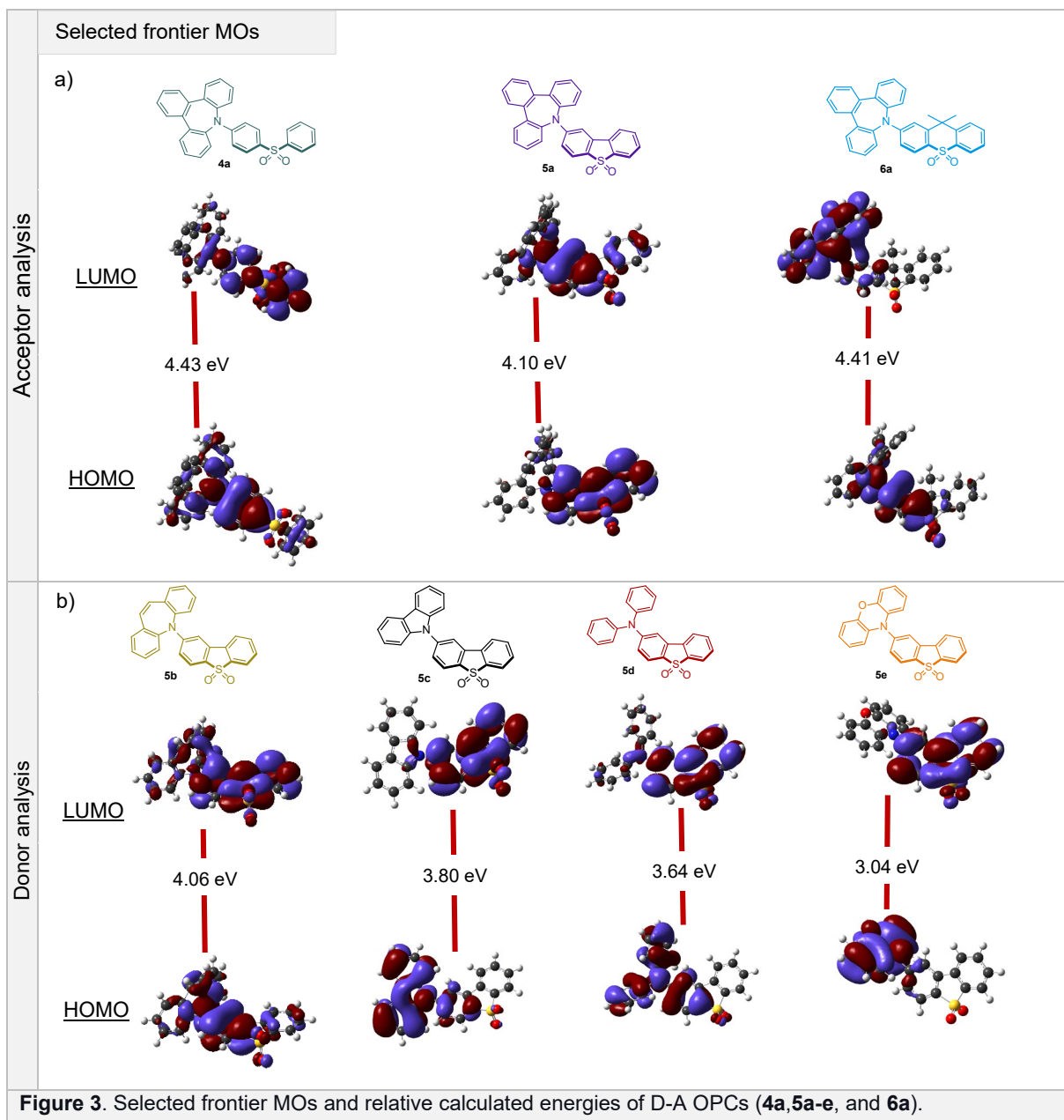
On the other hand, the fluorescence profile showed more differences in the analysis of the three members of the D-A family. Again, **5a** revealed a bathochromic effect compared with the less conjugated scaffolds. Interestingly, molecule **4a**, which has the most flexible acceptor core, exhibited a dual emission (DE) profile (Figure 2a). In this same compound, we did not observe changes in the absorption profile during the solvatochromism analysis (See Figure S4). However, the behavior was different in the fluorescence, showing significant changes in the ratio of the two bands involved in the DE (see Figure S3). The structural characteristics of compound **5a** conferred the biggest value in terms of Stokes shift parameter, indicating an increased excited state's charge transfer (CT) character (Table S1). Similarly, this behavior was observed experimentally in the solvatochromism study of the fluorescence using solvents with diverse polarities (see Figure S9). Indeed, the density functional theory (DFT) calculation performed at B3LYP/Def2TZVP Empirical Dispersion=GD3 level of theory showed the lowest value for the HOMO-LUMO energy gap in the compound **5a** as a consequence of the extended π conjugation compared with **4a** and **6a**. Interestingly, compound **6a**, which possesses the weakest sulfur-based acceptor, showed an inversion in the LUMO distribution, localizing it in the TBA core—this behavior of the named antiaromatic compound as an acceptor was previously reported (Figure 3a).[15]

The dibenzo[*b*,*d*]thiophene 5,5-dioxide (**5**) was selected for further investigation due to its red-shifted absorption and to evaluate the peculiar effect of the TBA donor unit (**a**). We next synthesized diverse D-A structures employing common nitrogen-donor widely used in material chemistry like carbazole (**c**), diphenylamine (**d**), and phenoxazine (**e**). Furthermore, we wanted to study the diverse or similar properties between the antiaromatic molecules **5a** and **5b**, in which the main difference is the presence of a third aromatic ring. According to the literature, the third benzene core presented in the TBA (**a**) distinguishes the conformations of structures **5a** and **5b** in the excited state, resulting in a planar conformation for **5b** and a bent conformation for **5a**.[15] This duality between planar and bent shapes is significant, as it contributes to the aromatic character that is acquired in the excited state by structures that are antiaromatic in the ground state. Intrigued by this diverse behavior, we wanted to investigate if this characteristic was important for the photocatalytic activity of these two molecules.

Analyzing the diverse absorption profiles, we can observe an increase in the red-shifted behavior related to the donor strength in compounds **5e**, **5d**, and **5c**. In contrast, the azepine-derived compounds are the most blue-shifted (Table 1, entry 5). The same trend is observed in the emission (Figure 2b). The Stokes shift values for the classical nitrogen donors (**c**, **d,** and **e**) demonstrate a more pronounced CT character with respect to **5a** and **5b** (Table 1, entry 8). This CT behavior is supported by the DFT studies, which suggested a better spatial separation between the HOMO and LUMO. As expected, the HOMO-LUMO energy gap followed a trend that is dependent on the electron-donating capacity of the nitrogen heterocycles and amine presented in compounds **5e** (3.04 eV), **5d** (3.64 eV)**,** and **5c** (3.80 eV). At the same time, **5a** and **5b** showed bigger values (4.10 eV and 4.06 eV, respectively) (Figure 3).

The strength of common donors plays a crucial role in influencing quantum yield (QY) measurements. As shown in Table 1, we observe a notable decrease in QY across the PCs **5e**, **5d**, and **5c**, with values of 39%, 35%, and 22%, respectively. The lowest values were obtained for molecules **5a** and **5b** (10% and 11%, each).
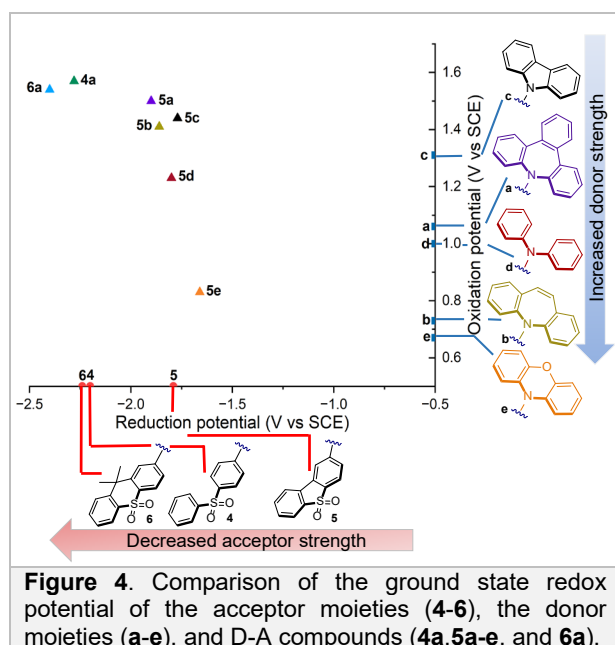
Remarkably, compound **5e** demonstrated minimal luminescence in nearly all solvents at room temperature. This behavior has been previously reported and is believed to be due to strong CT stabilization of the first excited state of the molecule.[16] This observation is further supported by the orthogonal D-A conformation calculated using DFT, which indicates a decoupled interaction between the HOMO and the LUMO (Figure 3b).

Figure 3. Selected frontier MOs and relative calculated energies of D-A OPCs (**4a**,**5a-e**, and **6a**).

Redox properties analysis.

We started our analysis looking at the impact of the diverse cores on the redox properties. Here, we can observe similar E_{ox} values ranging from 1.54 V to 1.66 V vs SCE. This behavior is consistent with preserving the same donor core (**a**) within the structure. In contrast, a significant difference was observed for the E_{red} values . By adjusting the acceptor strength of the sulfur core, we observed a trend where the D-A structure with the weakest acceptor (**6a**) yielded the most negative value (E_{red}= -2.4 vs SCE) (see SI, Table S1). In contrast, molecule **5a**, which has the strongest acceptor, displayed the most positive one (E_{red}= -1.9 V vs SCE).

We next investigated the diverse donors. For D-A molecules **5c**, **5d**, and **5e**, the redox potential calculated for the ground state is slightly more positive than the one measured for the single donor. For example, for phenoxazine (**e**) we measure an E_{ox}= 0.67 V, while for compound **5e** the E_{ox}= 0.83 V vs SCE. While, IMD (**b**) with an oxidation potential of 0.73 V when present in the D-A molecule **5b** resulted in a considerably different E_{ox} of 1.41 V (Figure 4).

Figure 4. Comparison of the ground state redox potential of the acceptor moieties (**4-6**), the donor moieties (**a-e**), and D-A compounds (**4a**,**5a-e**, and **6a**).

A molecule that in the excited state exhibits both strong oxidative power (E^*_{ox} up to -1.5 V) and strong reductive power (E^*_{red} up to 1.5 V) can be classified as a bimodal photocatalyst. This type of molecule is capable of driving both oxidative and reductive reactions, thereby offering significant versatility to achieve photocatalytic transformations. To our delight, molecule **5a** possesses an E_{ox}= 1.54 V vs SCE, which is the highest value among the entire family of donor-acceptor (D-A) compounds. In the same way, this molecule exhibits a promising E^*_{ox}=-1.76 V vs SCE (Table 1, entries 1 and 2). For E_{red}, **5a** maintains a good balance between the redox potentials in both the ground and excited states, showing values of E_{red}= -1.89 V and E^*_{red} = 1.41 V vs SCE (Table 1, entries 3 and 4). Comparing it with its analog **5b**, we observe similar redox potentials except for E_{ox} and E^*_{red} values.

The redox window is more limited for the other members of the D-A family. For example, for molecule **5e** the E_{ox} is 0.83 V and the reduction E_{red} is -1.66, which are the lowest values among all family members (Table 1, entries 1 and 3).

Table 1: Summary of the Excited- and Ground-State Photoredox properties[a]
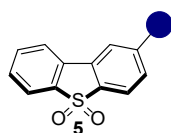
Entry	⬤ , PC	TBA, 5a	DBA, 5b	Carb, 5c	DPA, 5d	PHO, 5e
1	E_{ox} (V)	1.54	1.41	1.44	1.23	0.83
2	E^{*}_{ox} (V)	-1.76	-1.79	-1.66	-1.67	-1.77
3	E_{red} (V)	-1.89	-1.86	-1.7	-1.8	-1.66
4	E^{*}_{red} (V)	1.41	1.34	1.4	1.1	0.94
5	λ_{abs} (nm)	320	312	336	346	393
6	λ_{em} (nm)	430	441	493	525	564
7	$E_{0,0}$ (eV)	3.3	3.2	3.1	2.9	2.6
8	Stokes shift (nm)	110	129	157	179	171
9	τ (ns)	τ_1=1.6, τ_2=5	0.7	11.6	9.1	τ_1=3.3, τ_2=8.7
10	QY (%)	10	11	22	35	39
11	CT character	▭	▭	▭	▭	▭

[a]All potentials were measured in MeCN. Values are reported in V versus SCE (see SI). The colored bars qualitatively indicate the presence of a CT excited state–the color intensity is based on Stokes shift and solvatochromism of fluorescence. All the solvatochromism measurements were performed at room temperature except for compound **5e** (77K).
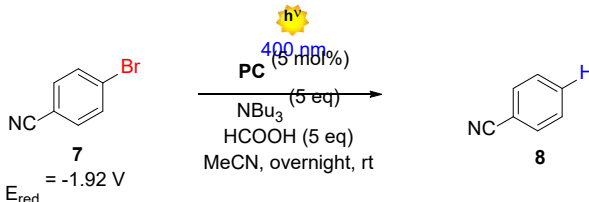
Photocatalytic studies and synthetic applications

After establishing structure-property relationships, we aimed to use the synthesized donor-acceptor (D-A) compounds to investigate their photocatalytic activity. We found that most members of the D-A family exhibited promising redox potentials in their excited states, indicating their potential to function as effective bimodal photocatalysts. Additionally, our photophysical characterization provided essential insights into their behavior in the excited state and stability. We initiated the study of the photocatalytic activity of all family members in an oxidative quenching cycle for the dehalogenation of 4-bromobenzonitrile (**7**). Typically, this type of chemical transformation requires higly reducing PCs or the use of UV light.[17] First, we evaluated the photocatalytic performance of molecules **4a**, **5a**, and **6a** (see SI, Table S3). As we expected, due to the blue-shifted absorption presented in molecules **4a** and **6a**, it was impossible to excite them under visible light (400 nm). Gratifyingly, PC **5a** delivered product **8** with a promising 63% NMR yield.

Next, we compare the photocatalytic behavior of compound **5a** with the other family members utilizing the same dehalogenation manifold. Here, even slightly changes in the redox properties have an influence on the yield of the reaction. The D-A with the azepine analog (**5b**), gave the dehalogenated product **8** in 58% NMR yield (Table 2,

entry 2). Quite surprisingly, **5e** showed only traces of **8**, even with an E^*_{ox} of -1.77 V (Table 2, entry 5).

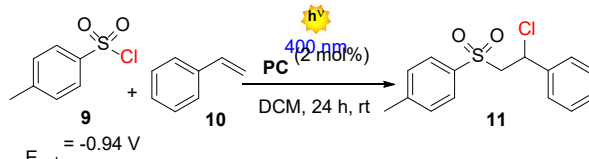**Table 2:** Dehalogenation of 4-bromobenzonitrile (**7**).

Entry	PC	^{1}H NMR Yield^a (%)
1	5a	63
2	5b	58
3	5c	56
4	5d	44
5	5e	Traces

^{a} CH$_2$Br$_2$ as internal standard

Under the oxidative quenching study, we also evaluated the photocatalytic potential of the new family of D-A compounds in the atom transfer radical addition (ATRA) reaction involving styrene and tosyl chloride (TsCl), as previously reported by Zysman-Colman and co-workers.[11] Compound **5e** showed the best performance with a 27% calculated NMR yield (20%, isolated yield) (Table 3, entry 3), while the azepine derivatives **5a** and **5b** led the transformation at 13 and 8%, respectively (Table 3, entries 1 and 2). However, these results are comparable to those obtained by the same author using the well-established PCs **1** and **3** (10% and 16%, respectively).

**Table 3:** ATRA reaction between tosyl chloride (**9**) and styrene (**10**).

Entry	PC	Yield^a %
1	5a	13
2	5b	8
3	5c	27 (20)
4	5d	12
5	5e	21

^{a} Yields determined by ^{1}H NMR analysis of the crude mixture using CH$_2$Br$_2$ as internal standard. Isolated yield in parenthesis.

Next, we wanted to analyze the use of the PCs in reductive quenching mechanisms. For this purpose, we selected the Giese-type addition between the N-Cbz-Pro **12** (E_{ox}= 0.95 V vs SCE) and the dimethyl maleate **13**, that is a standard benchmark reaction for the evaluation of novel PCs.[18] In this case, we obtained the best result using compound **5a** with an 76% NMR yield (65%, isolated yield) (Table 4, entry 1). Compound **5b** and **5c**, whose redox potential in the ground and excited state are

similar to **5a**, leads to the formation of the **14** in 59% and 65% NMR yield, each (Table 4, entries 2 and 3). Interestingly, compounds **5d** and **5e** showed the worst photocatalytic performances that can be attributed to their inferior E^*_{red} (Table 4, entries 4 and 5).

Table 4: Giese addition using N-Cbz-Pro (**12**) and dimethyl maleate (**13**).
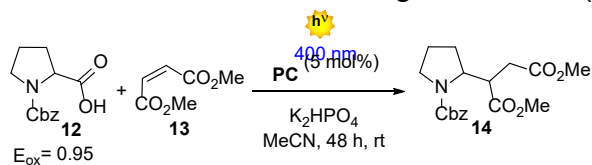
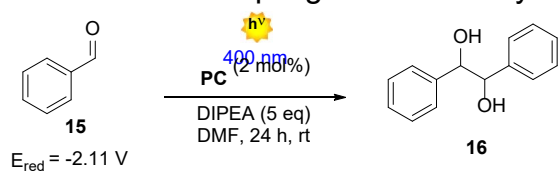| Entry	PC	Yield^a %
1	5a	76 (65)
2	5b	59
3	5c	65
4	5d	43
5	5e	5

^{a} Yields determined by ^{1}H NMR analysis of the crude mixture using CH_2Br_2 as internal standard. Isolated yield in parenthesis.

Furthermore, we obtained pleasing outcomes when we tried the photocatalyzed reductive pinacol coupling of benzaldehyde (**15**) , as reported by Rueping.[19] In this methodology, the reduction of compound **15** is facilitated by reduced photocatalyst (PC) and the interaction of **15** with the radical cation of DIPEA. The best result, again, was attributed to molecule **5a** with a 60% of isolated yield (Table 5, entry 1). In contrast, molecule **5b** showed the worst performance with 41% NMR yield (Table 5, entry 2). For compounds **5c-e** , the NMR yield calculated for product **16** was similar (55-51%), probably due to the comparable reductive properties in both ground and excited states (Table 5, entries 3,4 and 5).

Table 5: Pinacol coupling of benzaldehyde (**15**).

Entry	PC	Yield^a %
1	5a	69 (60)
2	5b	41
3	5c	55
4	5d	51
5	5e	51

^{a} Yields determined by ^{1}H NMR analysis of the crude mixture using CH_2Br_2 as internal standard and refers to the combined yield of meso:dl isomers. Isolated yield in parenthesis.

Conclusion

In conclusion, we explored the potential of tribenzo[b,d,f]azepine (TBA) as a donor in donor-acceptor (D-A) organic photocatalysts (PCs). We synthesized a new series of sulfur-based D-A compounds and compared their photophysical and photoredox properties with TBA, its analog 5H-Dibenz[b,f]azepine (IMD), and common nitrogen donors. The excited state redox potentials of these compounds suggest their suitability for challenging photocatalytic reactions. TBA showed a well-balanced redox window, making it a promising candidate for new PC designs. While TBA and IMD displayed similar characteristics, IMD's shorter lifetime proved unfavorable in photocatalytic tests. The differing excited state conformations (bend vs planar) of these benzodiazepine analogs did not negatively impact photocatalytic activity. This study suggests that antiaromatic compounds like TBA could replace traditional nitrogen donors in PCs, offering new opportunities for photocatalysis.

Supporting Information

Supporting Information File 1: Reactivity studies, general experimental procedures, product isolation and characterization, spectroscopic data for new compounds, and copies of NMR spectra.

Acknowledgements

Funding

References

1. a) Romero, N. A.; Nicewicz, D. A. *Chem. Rev.,* **2016**, *14*, 10075–10166. b) Bortolato, T.; Cuadros, S.; Simionato, G.; Dell'Amico, L. *Chem. Commun.,* **2022**, *58*, 1263–1283. c) Haria, D. P.; König, B. *Chem. Commun.,* **2014**, *50* , 6688–6699.

2. Vega-Peñaloza, A.; Mateos, J.; Companyó, X.; Escudero-Casao, M.; Dell'Amico, L. *Angew. Chem. Int. Ed.*, **2021**, *60*, 1082–1097.

3. Bryden, M. A.; Zysman-Colman, E. *Chem. Soc. Rev.*, **2021**, *50*, 7587–7680.

4. Uoyama, H.; Goushi, K.; Shizu, K.; Nomura, H.; Adachi, C. *Nature,* **2012**, *492*, 234–238.

5. Shang, T. Y.; Lu, L. H.; Cao, Z.; Liu, Y.; He, W. M.; Yu, B. *Chem. Commun.,* **2019**, *55*, 5408–5419.

6. Speckmeier, E.; Fischer, T. G.; Zeitler, K. *J. Am. Chem. Soc.,* **2018**, *140*, 15353–15365.

7. For general examples see: a) Yang, S. Y.; Tian, Q. S.; Yu, Y. J.; Zou, S. N.; Li, H. C.; Khan, A.; Wu, Q. H.; Jiang, Z. Q.; Liao, L. S. *J. Org. Chem.,* **2020**, *85*, 10628–10637. b) Zhang, Q.; Li, B.; Huang, S.; Nomura, H.; Tanaka, H.; Adachi, C. *Nat. Photonics,* **2014**, *8*, 326–332. c) Gudeika, D.; Lee, J. H.; Lee, P. H.; Chen, C. H.; Chiu, T. L.; Baryshnikov, G. V.; Minaev, B. F.; Ågren, H.; Volyniuk, D.; Bezvikonnyi, O.; Grazulevicius, J. V. *Org Electron.,* **2020**, *83, 105733.* d) Bezvikonnyi, O.; Gudeika, D.; Volyniuk, D.; Mimaite, V.; Sebastine, B. R.; Grazulevicius, J. V. *J. Lumin.,* **2019**, *206*, 250–259. e) Zhang, D.; Wei, H.; Wang, Y.; Dai, G.; Zhao, X. *Dyes and Pigments,* **2020**, *174*, 108028. f) Dos Santos, P. L.; Chen, D.; Rajamalli, P.; Matulaitis, T.; Cordes, D. B.; Slawin, A. M. Z.; Jacquemin, D.; Zysman-Colman, E.; Samuel, I. D. W. *ACS Appl. Mater. Interfaces,* **2019**, *11*, 45171–45179.

8. a) Jia, X.; Han, W.; Xue, T.; Zhao, D.; Li, X.; Nie, J.; Wang, T., *Polym. Chem.* **2019**, *10*, 2152–2161. b) Zhou, H.; Huang, Q.; Liu, X.; Xu, D.; Zhang, W.; Fu, S.; Feng, X.; Zhang, Z. *Dyes and Pigments,* **2021**, *184*, 108868.

9. Singh, V. K.; Yu, C.; Badgujar, S.; Kim, Y.; Kwon, Y.; Kim, D.; Lee, J.; Akhter, T.; Thangavel, G.; Park, L. S.; Lee, J.; Nandajan, P. C.; Wannemacher, R.; Milián-Medina, B.; Lüer, L.; Kim, K. S.; Gierschner, J.; Kwon, M. S. *Nat. Catal.,* **2018**, *1*, 794–804.

10. Song, Y.; Kim, Y.; Noh, Y.; Singh, V. K.; Behera, S. K.; Abudulimu, A.; Chung, K.; Wannemacher, R.; Gierschner, J.; Lüer, L.; Kwon, M. S. *Macromolecules,* **2019**, *52*, 5538–5545.

11. Bryden, M. A.; Millward, F.; Matulaitis, T.; Chen, D.; Villa, M.; Fermi, A.; Cetin, S.; Ceroni, P.; Zysman-Colman, E. *J. Org. Chem.,* **2023**, *88*, 6364–6373.

12. For the study of the effects of different donors in emitters see: a) Wang, C.; Zhao, Y.; Su, R.; Li, D.; Guo, Y.; Su, W.; Yu, T. *Dyes and Pigments,* **2022**, *208*, 110880. b) Tian, X.; Yao, M.; Liang, X.; Zhou, C.; Xiao, S.; Gao, Y.; Liu, H.; Zhang, S. T.; Yang, B. *Dyes and Pigments,* **2022**, *205*, 110463. c) Wu, Q.; Li, J.; Liu, D.; Mei, Y.; Liu, B.; Wang, J.; Xu, M.; Li, Y. *Dyes and Pigments,* **2023**, *217*, 111421.

13. a) Lei, B.; Huang, Z.; Li, S.; Liu, J.; Bin, Z.; You, J. *Angew. Chem. Int. Ed.,* **2023**, *62*, e202218405. b) Wu, Y.; Liu, X.; Liu, J.; Yang, G.; Han, S.; Yang, D.; Cao, X.; Ma, D.; Bin, Z.; You, J. *Mater. Horiz.,* **2023**, *10*, 3785–3790. c) Xiao, X.; Lei, B.; Wu, D.; Bin, Z. *Chem. Commun.,* **2023**, *59*, 6556–6559. d) Mamada, M.; Aoyama, A.; Uchida, R.; Ochi, J.; Oda, S.; Kondo, Y.; Kondo, M.; Hatakeyama, T. *J. Adv. Mat.,* **2024**, *36*, 202402905. e) Chen, Y. K.; Lei, J.; Wu, T. L. *Chem. Sci.* **2024**, *15*, 10146–10154.

14. a) Wang, Z.; Wang, Z.; Lu, P.; Wang, Y. *Chem. Asian J.* **2020**, *15*, 3519–3526. b) Yu, L.; Wu, Z.; Xie, G.; Luo, J.; Zou, Y.; Ma, D.; Yang, C. *J. Mater. Chem. C. Mater.,* **2020**, *8*, 12445–12449. c) Bezvikonnyi, O.; Gudeika, D.; Volyniuk, D.; Rutkis, M.; Grazulevicius, J. V. *Dyes and Pigments*, **2020**, *175,* 108104. d) Silva,

W. de P.; Decarli, N. O.; Espíndola, L.; Erfurt, K.; Blacha-Grzechnik, A.; Pander, P.; Lapkowski, M.; Data, P. *J. Mater. Chem. C. Mater.,* **2023**, *11*, 15246–15260.

15. Chen, Y.; Tseng, S. M.; Chang, K. H.; Chou, P. T. *J. Am. Chem. Soc.,* **2022**, *144*, 1748–1757.

16. Data, P.; Pander, P.; Okazaki, M.; Takeda, Y.; Minakata, S.; Monkman, A. P. *Angew. Chem.,* **2016**, *128*, 5833–5838.

17. Discekici, E. H.; Treat, N. J.; Poelma, S. O.; Mattson, K. M.; Hudson, Z. M.; Luo, Y.; Hawker, C. J.; De Alaniz, J. R. *Chem. Commun.,* **2015**, *51*, 11705–11708.

18. Mateos, J.; Rigodanza, F.; Vega-Peñaloza, A.; Sartorel, A.; Natali, M.; Bortolato, T.; Pelosi, G.; Companyó, X.; Bonchio, M.; Dell'Amico, L. *Angew. Chem. Int. Ed.,* **2020**, *59*, 1302–1312.

19. Nakajima, M.; Fava, E.; Loescher, S.; Jiang, Z.; Rueping, M. *Angew. Chem.,* **2015**, *127*, 8952–8956.